A Sensorless Closing Control for an AC Contactor Based on a New Armature Displacement Estimator

CHIEH-TSUNG CHI
Department of Electrical Engineering
Chienkuo Technology University
No. 1, Chieh Shou N. Rd., Changhua City 500, Taiwan, R.O.C
E-mail: jih@cc.ctu.edu.tw

Abstract: - This paper presents a new approach to solve the contact bounce after contacts closing problem for prolonging the lifespan and improving operation reliability. Based on combining a armature displacement estimator (ADE) with a simple hysteresis controller, such that the coil-current difference between the ac electromagnetic contactor (abbreviated ac contactor) body and the estimator is minimized, the proposed method overcomes the installation of an armature displacement measuring mechanism is indispensable restrictions imposed by previously described closing control methodologies. By using the proposed algorithm, an efficient control configuration can be obtained to reduce bounce duration. Computer simulations, of the proposed method, illustrate lots of benefits that are provided by proposed sensorless closing control configuration.

Key-Words: - Contact bounce, Estimator, Hysteresis controller, Armature displacement, Sensorless, AC electromagnetic contactor.

1 Introduction

Currently, a large number of contactors have widely used in industrial switchgear equipments [1-3]. Most of them are applied in the power transmission and control systems for making/opening the power source of load. When contactor is applied to a voltage source, the input electrical energy is converted into the mechanical energy for doing work to armature. In many cases, since the armature of contactor with too much kinetic energy at the contacts closing instant, this result leads to an inelastic collision between contacts. Consequently, resulting in an uncertain number of rebounds after the first touch could be produced before they reach a permanent state of contact. If the contactor is specified to work in the AC3 category, the starting current of load generally is about 6-10 times of the rated load current, such as the starting current of induction motor and the switching an uncharged capacitor in parallel with a charged capacitor bank [4]. Supposed that contactor is utilized in three phase system, as result of the contact bounces and starting current occurs at the same time, arcing with high temperature must be harmful to the contacts of contactor.

The contact bounces with erosion have been thoroughly investigated in the past [4-6]. Many authors have discussed the contact bouncing problems related to the reduction of bounce duration after contacts closing by using numerous methodologies [7,13-18]. For example, Nouri et al. first reported the production of contact bounce that is caused by the excessive kinetic energy prior to two contacts impact. Therefore, Nouri et al. proposed a new approach for the reduction of the kinetic energy of armature. According to the armature displacement, they effectively controlled the kinetic energy of armature by using the power electronic technology [8]. In addition, Li et al. made use of experimental method; they found that if user purposely selects the closing phase angle of ac voltage source to energize the ac contactor, a minimized kinetic energy was derived [9]. Later, related to searching an optimal closing phase angle has been taken as optimization problem by Su et al. [10]. In a similar manner, Zhang [11] presented that if the ac contactor can be energized at the moment of the zero crossing point of load current, in theory, even if contact bounce occurs, there is no any energy dissipated between two contacts. Therefore, no influence on the lifespan of contact is obtained.

Although many studies have been published concerning the reduction of contact bounce, no matter which they use open- or close-loop method to control the closing process of ac contactor. In general, the dynamic armature-displacement data must be provided to their system controller. To achieve this goal, it is essential to arrange a proper measuring sensor on the contactor mechanism. Several critical drawbacks are then produced, such that armature mass becomes heavier, manufacturing cost becomes inexpensive, and the using durability is shortened. In recent years, Espinosa et al. [12] presented a close-loop method to control the kinetic energy that acts on armature during closing process based on estimation method.

A new dynamic ADE is proposed in this paper. With application of both the coil voltage and the coil current values, the dynamic armature displacement can be estimated by proposed calculation algorithm. Feasibility and robustness of the proposed ADE are validated through several experimental and simulation tests. The developed ADE was again combined with a hysteresis controller to implement the objective of contact bounce control during closing process. The methods reported here could be beneficial to research attempting to increase the performance of contactors.

2 Structures and Energy Conversion

Fig. 1 shows the basic configuration of a typical ac contactor. The ac contactor is generally seemed as an electromechanical system and composed of three parts, such as the electrical system, lossless magnetic energy-conversion system and mechanical system. Included facilities of the electrical system are the applied voltage source, current-carrying conductor and exciting coil. It is responsible for providing the energy to the magnetic energy conversion system. Magnetic energy-conversion system is composed by the movable core, stationary core and air gaps between the cores. For this type of system the magnetic field serves as the coupling medium between electrical system and mechanical system. On one hand, the input electrical energy is converted into coupling field, and on the other hand, part of energy is further transferred to the mechanical system for moving the armature. The mechanical system consists of an armature, one or triple sets of contacts, return springs and contacts' springs. It is responsible for managing the transferred energy from the magnetic energy-conversion system and moving the armature if the strength of magnetic force is larger than the spring tension force.

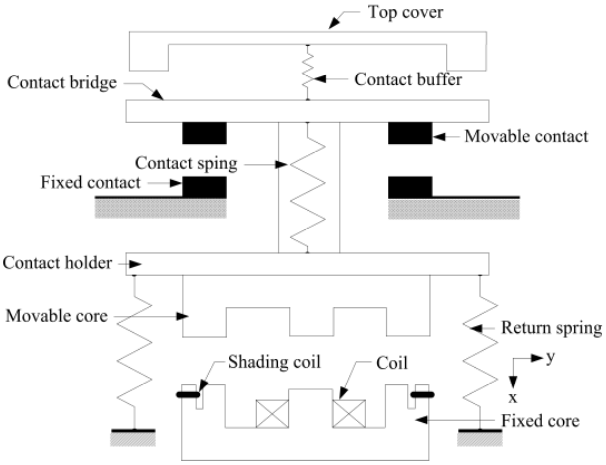

Fig. 1. Shows the basic configuration of an ac contactor.

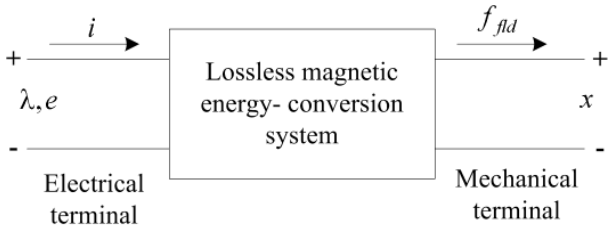

Fig. 2. Lossless magnetic energy-conversion system is represented as two-port element.

2.1 Energy Conversion

When a contactor is energized by a voltage source, part of the input electrical energy will be stored in lossless magnetic energy storage system, part of which is dissipated in heat form, and part of which be converted into mechanical energy. For brevity, the contactor may be assumed to be a magnetic field-based electromechanical energy-conversion device, the loss mechanisms can be represented by external elements connected to these terminals. Thus, the contactor can be simply represented as a lossless magnetic energy-conversion system with electrical and mechanical terminals, as shown in Fig. 2. With reference to the Fig. 2, the relations between the electrical system, magnetic energy-conversion system and mechanical system can be expressed as shown below:

$$dW_{elec} = dW_{mech} + dW_{fld} \quad (1)$$

where，

dW_{elec} =differential electric-energy input,

dW_{mech} =differential mechanical-energy output,

dW_{fld} =differential change in magnetic stored

energy.

Indeed, the input electrical energy supplied from the voltage source can be written as follows:

$$dW_{elec} = e\, i\, dt \tag{2}$$

By applying the Faraday's law, the induced voltage across the coil e can be represented in terms of the flux linkage λ as

$$e = \frac{d\lambda}{dt} \tag{3}$$

For convenience, the magnetic energy-conversion system can be assumed to be a lossless and conservative. This means the energy stored in coupling fields is a function of the state of the electrical and mechanical variables. In fact, to minimize the hysteresis and eddy losses, the ferromagnetic material is purposely selected and arranged in laminations. Therefore, the flux flows through the cores can be assumed the same as that of the air gap. It varies proportionally with the coil current. In other words, the flux linkage λ and the coil current i are considered to be linearly related by a factor which depends solely upon the geometry and hence the armature position x.

$$\lambda = L(x)i \tag{4}$$

Equation (4) points out the magnetic circuit can be described by an inductance L which is a function of the geometry of the magnetic structure and permeability of the magnetic material.

2.2 Electromagnetic Force

Assuming work done by the electromagnetic force f_{fld} is defined as energy transfer from coupling fields to mechanical system dW_{mech}, it is given by

$$dW_{mech} = f_{fld}\, dx \tag{5}$$

Substituting (3) and (5) into (1), we get

$$dW_{fld} = id\lambda - f_{fld}\, dx \tag{6}$$

Since the magnetic energy-conversion system is lossless and conservative, hence, the value of W_{fld} can be uniquely specified by the independent variables λ and x.

Substitutes (4) into (6) and for a specified armature displacement x, that is $dx = 0$. The representation of the coupling energy W_{fld} can be given by the following form:

$$\begin{aligned} W_{fld} &= \int_0^{\lambda} \frac{\zeta}{L(x)}\, d\zeta \\ &= \frac{\lambda^2}{2L(x)} \end{aligned} \tag{7}$$

where ζ is the dummy variable of integration. Since $i(\lambda, x) = \lambda / L(x)$, the other form of (7) is expressed as follows:

$$W_{fld} = \frac{1}{2} i^2 L(x) \tag{8}$$

The W_{fld} is a state function and determined uniquely by the values of the independent state variables λ and x.

$$dW_{fld}(\lambda, x) = \frac{\partial W_{fld}}{\partial \lambda} d\lambda + \frac{\partial W_{fld}}{\partial x} dx \tag{9}$$

Equation (9) is compared with (6) yields

$$f_{fld} = -\frac{\partial W_{fld}(\lambda, x)}{\partial x} \tag{10}$$

The electromagnetic force f_{fld} acts on armature can be determined by using (10). Alternatively, one can use a state function other than energy, namely, the coenergy, to obtain the magnetic force directly as a function of current.

$$W'_{fld}(i, x) = i\lambda - W_{fld}(i, x) \tag{11}$$

Taking the derivative of the first term in the right side of (11), yields

$$d(i\lambda) = id\lambda + \lambda di \tag{12}$$

Substitution of (6) and (12) into (11), results in

$$dW'_{fld}(i, x) = \lambda di + f_{fld}\, dx \tag{13}$$

Coenergy, $W'_{fld}(i,x)$, means that is a function of the two independent variables i and x. Thus, its derivative with respect to these independent variables is derived and presented as follows:

$$dW'_{fld}(i,x) = \frac{\partial W'_{fld}}{\partial i} di + \frac{\partial W'_{fld}}{\partial x} dx \tag{14}$$

Equations (13) and (14) must be equal for all the coefficients of di and dx; thus

$$f_{fld} = \frac{\partial W'_{fld}}{\partial x} \tag{15}$$

Equation (15) means the electromagnetic force acts on armature that can be further written by the derivative of coenergy representation as shown below:

$$\begin{aligned} f_{fld} &= \frac{\partial W'_{fld}}{\partial x} \\ &= \frac{1}{2} i^2 \frac{dL(x)}{dx} \end{aligned} \tag{16}$$

3 Closing Process Analysis

Fig. 3 shows the typical configuration of an electromagnetic contactor. The electrical system is merely represented by a voltage source $u(t)$ and a fixed resistor r. Based on Kirchhoff's voltage law, the voltage equation in electrical system may be expressed as follows:

$$u(t) = ir + \frac{d\lambda}{dt} \tag{17}$$

Since the flux linkage λ can be expressed as (4), it is substituted into (17) and results in

$$u(t) = ir + L(x)\frac{di}{dt} + i\frac{dL(x)}{dt}\frac{dx}{dt} \tag{18}$$

The term $L\,di/dt$ is the self-inductance voltage term and the term $i(dL/dx)(dx/dt)$ is the velocity-voltage term, which is responsible for the energy transfer between the external electrical system and lossless magnetic energy-conversion system.

In the mechanical system, m represents the armature mass while the spring and damper are represented by a spring constant K and a damping coefficient D, respectively. The armature displacement x_0 is the equilibrium position of the mechanical system where the armature is at opening position Similarly, the dynamic behavior of the translational mechanical system can be described by Newton's motion law, so that

$$f = m\frac{d^2x}{dt^2} + D\frac{dx}{dt} + K(x - x_0) - f_{fld} \tag{19}$$

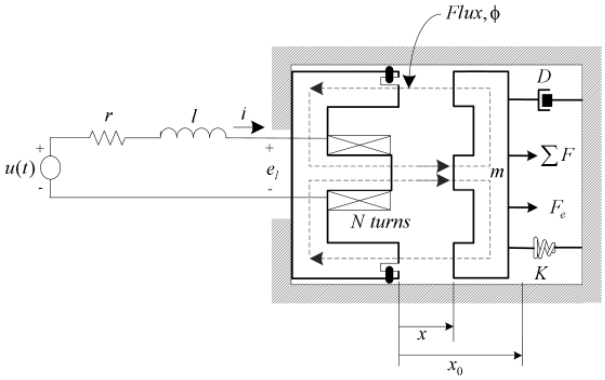

Fig. 3. Sketches all the subsystems of a typical ac contactor.

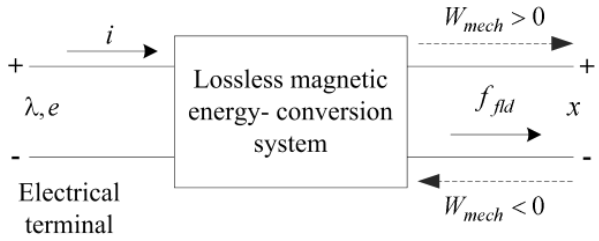

Fig. 4. Energy transfer of ac contactor in both motoring and generatoring modes.

To make use the principle of energy conservation, Fig. 4 shows that the lossless electromechanical energy-conversion system intervenes between the electrical system and the mechanical system. It served as the coupling medium between these two systems. Energy transferred direction of the mechanical energy is determined by the moving direction of the armature. If the mechanical energy is positive, it represents that the armature engaged with the fixed core and the contactor fulfils the motor action; on the contrarily, if the mechanical energy is negative, it represents that the armature disengaged from the fixed core, and the contactor performs the generator action. Moreover, there is another important result can be deduced from (5)

$$\begin{aligned} W_{mech} &= -\int_x^{x_0} f_{fld}\, dx \\ &= \int_{v_0}^{v} mv\, dv \\ &= \frac{1}{2}mv^2 - \frac{1}{2}m{v_0}^2 = \Delta E_k \end{aligned} \tag{20}$$

Equation (20) indicates the work done by the electromagnetic force equals the change in the kinetic energy of the armature. Indeed, (20) is commonly referred to as the work-energy theorem [19]. The symbol ΔE_k represents the differential kinetic energy of the armature during the considered armature displacement period. In the Fig. 3, x_0 and v_0 indicates the initial displacement and velocity of the armature, respectively; let x and v be the instantaneous armature displacement and moving velocity, and $x < x_0$. In case of the armature displacement and moving velocity at the moment of two contacts impact are taken as the final displacement and velocity in (20). It is more clearly depicted that total amount of the kinetic energy or moving velocity with contacts prior to impact may properly be controlled by means of the electromagnetic force. In the closing process, the coil current generally varies exponentially with the value of ac voltage source. For an AC contactor, the relationship between the coil current and the flux is linear and the representation can be represented as follows:

$$\phi = \frac{\sqrt{2} N I}{x_l / \mu_0 \mu_r S} \cos(wt) \tag{21}$$

Since the flux linkage $\lambda(i, x) = L(x)i = N\phi$ and coil inductance varies inversely proportional to the total reluctance value $R(x)$, thus, the magnetic force, which has represented as shown (16), could be derived in another form

$$\begin{aligned} f_{fld} &= \frac{1}{2}\phi^2 \frac{dR(x)}{dx} \\ &= \frac{\phi^2}{2\mu_0 S} \end{aligned} \tag{22}$$

where, the relevant symbols in (21) and(22) are defined as follows:

$R(x)$: the reluctance in the magnetic circuit,

μ_0 : the absolute permeability in the air, equal to $4\pi \times 10^{-7}\ H/m$

N : a number of windings in the coil,

I : the rms current-carrying coil,

x_l : the average length of the magnetic circuit,

μ_r : the relative permeability of the coil substances

S : the cross-sectional area of the air gap,

ϕ : the instantaneous flux.

Obviously, (22) shows the electromagnetic acts on the armature during closing process is determined by the square of the coil current or the flux strength in the magnetic circuit [11]. In a word, the kinetic energy with armature before contacts closing actually can be achieved by controlling the value of applied coil voltage.

4 Sensorless Armature Displacement Estimator (ADE)

Based on the work-energy theorem, as can be seen in (20), the kinetic energy in armature during closing process can be effectively controlled by changing the applied voltage source value. Fig. 5 shows an overall close-loop block diagrams for an ac contactor by using sensorless closing control method. The resultant force between electromagnetic force and spring anti-force f_{error} and the armature displacement x are served as the input variables of the hysteresis controller [20,21]. The upper and lower limit force error is automatically determined by the armature displacement. The output of the hysteresis controller is again integrated with a pulse width modulation generator to control the applied voltage source value. In addition to the kinetic energy in armature before contacts closing is considered, it is essential to shorten the total closing time as possible as. To attain above-mentioned goals, the closing process of ac contactor is divided into three subdivisions, such as acceleration region, deceleration region and holding region. The first stage is acceleration region in which the ac contactor is applied by the maximum allowable voltage in order to shorten the responding time; the second stage is deceleration region, this region generally starts prior to the contacts closing till that the cores are closed together. The third stage means that the armature has engaged with the fixed core. If an energy-saving objective is taken into consideration, the ac contactor is needed to be applied a coil voltage value as long as it can continue to hold armature closed with fixed core.

In Fig. 5, the curve of the spring anti-force f_f with respect to the armature displacement is used as force command, which is determined by experimental approach. Therefore, the proposed control strategy can also be called as a counter-force tracing method. The electromagnetic force f_{fld} acts on the armature is dynamic calculated from the coil-current value and the estimated armature displacement. The force error f_{error} between the reference spring anti-force and

the electromagnetic force is obtained and fed to the hysteresis controller as input variable.

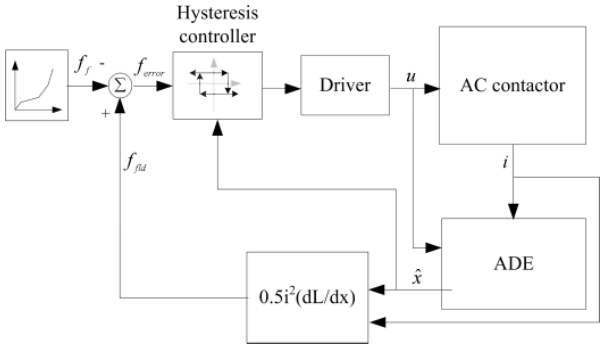

Fig. 5. Sketches overall block diagram for the sensorless closing control of an ac contactor.

4.1 Coil-Voltage Sensory Circuit

In the close-loop closing control system shown in Fig. 5, the coil voltage is applied form a step-down buck converter. The coil is directly connected with a power MOSFET in series. By timing the energizing period of the power MOSFET, a wide allowable range of coil voltage can be obtained from the rectified dc voltage of the full-bridge circuit, as shown in Fig. 6. The more duty cycle of driving signal has, the larger applied coil voltage is. The coil-voltage sensory circuit is connected with the system control board in parallel. The dynamic coil voltage can be sampled and justified by the microcontroller-based control board. The sampled coil voltage with respect to the reference voltage level V_- is symbolized as V_o.

For satisfying with the electrical specification of ac contactor, the applied coil voltage should be limited within 85% to 110% of the rated voltage. Fig. 6 shows that the coil voltage is measured by using two resistors, R_y and R_x. By employing the voltage division law, the coil voltage V_o with respect to the reference voltage level V_- can be calculated as shown below.

$$V_o = \frac{R_x}{R_x + R_y} * V_+ \tag{23}$$

Therefore, the positive terminal of the rectified dc voltage V_+ or the external ac voltage source U_{AC} or dc voltage source U_{DC} can be easily deduced from the formulas shown in (23).

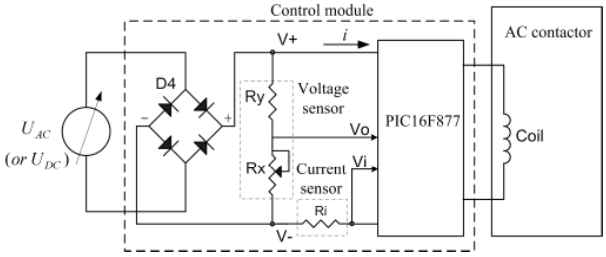

Fig. 6. Demonstrates the sensory circuit of both the coil voltage and the coil current.

4.2 Coil-Current Sensory Circuit

For estimating the armature displacement and completing the sensorless closing control of an ac contactor, in addition to the coil voltage, the coil current is needed to be detected as well. As the sketch of the control mechanism indicated in Fig. 6, a coil-current sensor R_i is made by a resistor with fixed resistance. This coil-current sensor features better temperature characteristics. Its key electrical specifications are listed in Table 1. This coil-current sensor is connected with the coil in series. During closing process, the voltage across the coil-current sensor R_i, V_i. Furthermore, make use of the ohmic law, the dynamic current flows through coil can be simply calculated by $i = V_i / R_i$.

Table 1. Electrical specifications of current sensor (LRB0805)

Parameters	Ratings	units
Max. value	4.5	A
Resistance	20	$m\Omega$
Tolerance	$J: \pm 5$	%
Thermal coefficient	± 100	$ppm/^oC$
Environmental temperature	+ 70	^oC
Operating temperature	– 40 ~ +155	^oC

4.3 Armature Displacement Estimator

To implement the proposed sensorless closing control of an ac contactor, as shown in Fig. 5, the upper and lower force error limitation of hysteresis controller should be automatically regulated by the armature displacement. A new method is proposed to obtain the dynamic armature displacement by software calculation and acted as the input variable of system controller. Some critical disadvantages imposed by the previously method will not be

produced again and it is cost-effective. The structure of this new ADE is diagramed in Fig. 7.

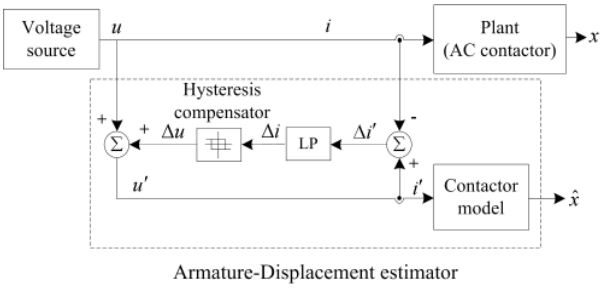

Fig. 7. Sketches the structure of new proposed ADE.

In many applications, the coil current is commonly incorporated into a large amount of disturbances, so that the coil-current difference $\Delta i'$ shown in Fig. 7 need to be first filtered by a low-pass filter. In addition, let ac contactor be supplied with a voltage $u(t)$. The input-output mapping relation between the applied voltage $u(t)$ and the armature displacement x can be expressed as follows:

$$u : \Im \Rightarrow x \tag{24}$$

Likewise, the mapping relation between the applied voltage of contactor model u' and the estimated armature displacement $\hat{x}$ can also be written as follows:

$$u' : \Im' \Rightarrow \hat{x} \tag{25}$$

The main designing goal of the armature displacement can be described in the following form

$$\lim_{t\to\infty}[x(u) - \hat{x}(u')] = 0 \tag{26}$$

Let the moving velocity of armature be defined as the derivative of armature displacement with respect to time $v = dx/dt$, the mesh voltage equation in the electrical system, as seen in (18), can be rewritten as

$$\underbrace{L(x)\frac{d\,i}{d\,t}}_{1} + \underbrace{i\,v\frac{d\,L}{d\,x}}_{2} + \underbrace{r i}_{3} = u(t) \tag{27}$$

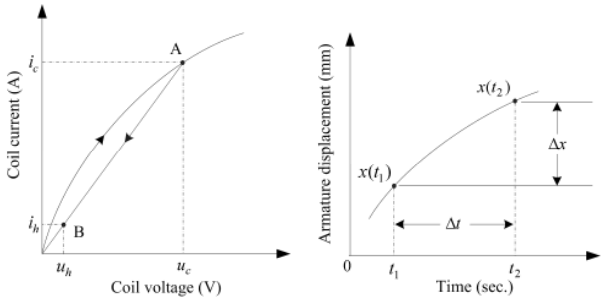

(a) (b)

Fig. 8. During closing process, (a) part of the coil current with respect to the coil voltage curve, and (b) part of armature displacement curve.

During closing process, part of the typical coil voltage with respect to the coil current and the time-varying armature displacement curve are illustrated in Fig. 8. It is noteworthy at the time instant t_1 and t_2 , Fig. 8(b) depicts the corresponding armature displacement are $x(t_1)$ and $x(t_2)$, respectively. Let us consider the time difference $\Delta t = t_2 - t_1$. In case of the time difference Δt is approach to zero. Corresponding armature displacement $x(t_1)$ at time instant t_1 is very closely to the corresponding armature displacement at time instant t_2 , thus results in $x(t_1) \approx x(t_2)$. Moreover, the coil inductance inherently is a function of the armature displacement, hence, we obtain $L(x(t_1)) \approx L(x(t_2))$. The velocity voltage in the electrical system model becomes

$$\lim_{\Delta t\to 0}[e(t_2) - e(t_1)] = 0 \tag{28}$$

Equation (28) means that there is no velocity voltage across the coil instantaneously. The second term of (27) can be defined as

$$R_1 \equiv v\frac{d\,L}{d\,x} \tag{29}$$

Substituting (29) into (27), we obtain

$$L\frac{d\,i}{d\,t} + R\,i = u(t) \tag{30}$$

where the generalized resistance R is defined as $(r + R_1)$, thus the solution of the coil current must has the exponential form and can be represented as

$$i(t) = \frac{E}{R}(1 - e^{-\frac{R}{L}t}) \tag{31}$$

Apparently, the coil current exponentially varies with the applied coil voltage. Furthermore, (31) indicates the coil current is directly controlled by the applied coil voltage. As seen in Fig. 7, the measured coil current i and the estimated coil current are together sampled and compared, let their difference be defined as

$$\Delta i = i' - i \tag{32}$$

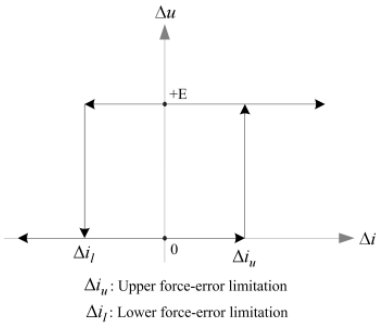

Fig. 9. Sketches the operation algorithm of hysteresis comparator in armature displacement estimator.

If the armature displacement of the contactor, x, is different from that of the estimator, $\hat{x}$, the coil current difference Δi will be produced and served as the input variable of hysteresis comparator, which is programmed as shown in Fig. 9, and output a compensation voltage Δu for offsetting the applied coil voltage of estimator. Therefore, the final estimated armature displacement trajectory $\hat{x}$ is always tracing the armature displacement change of ac contactor.

5 Laboratory Tests and Discussions

The objective of the present experiment is to investigate the sensorless closing control of ac contactor. A dynamic armature displacement is commonly needed. It is produced by the proposed ADE. According to the instantaneous value of the armature displacement, the closing process is partitioned into three operating regions, such as acceleration region ($0 < x \le x_i$), deceleration region ($x_i < x \le x_j$), and holding region ($x > x_j$), as shown in Fig.10. Notice that the direction definition in armature displacement is defined as a positive direction when the armature-displacement moving right, that is the armature moved back the fixed core. However, for convenient observation, the moving direction of armature will be re-defined as positive direction when the contactor acts as motor action or carries out closing process.

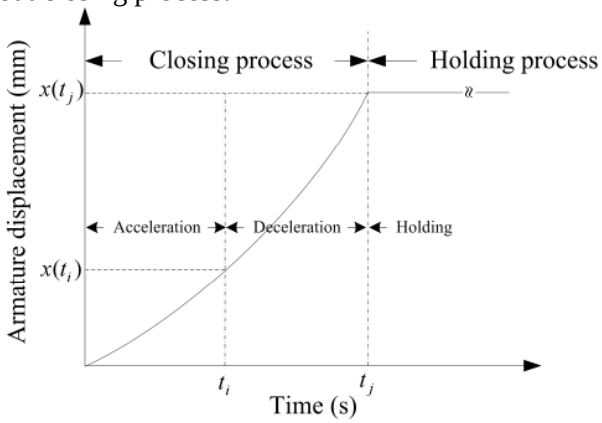

Fig. 10. Divides the closing process into three operating subdivisions.

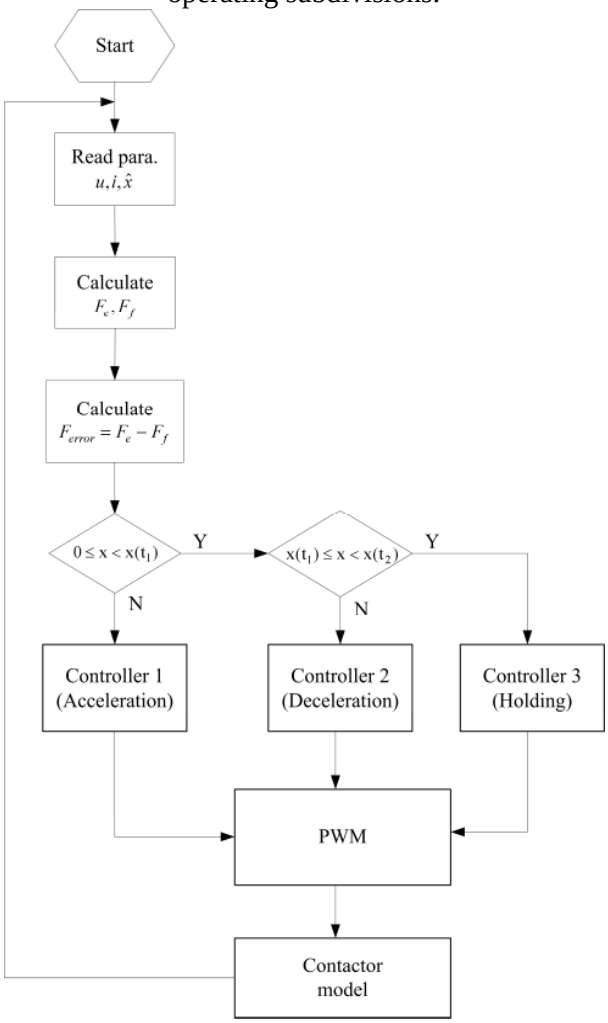

Fig. 11. The algorithm is used to the proposed sensorless close-loop closing control of an ac contactor.

The complete close-loop sensorless closing control algorithm is diagrammed in Fig. 11. First, the coil voltage, the coil current, and the estimated armature displacement are sampled by the system controller. According to the armature displacement, the corresponding spring anti-force and the coil

inductance are obtained by using look-up table method. Next, the dynamic electromagnetic force acts on the armature is calculated. Further, along with the force error $f_{error} = f_{fld} - f_f$ is obtained and integrated with the armature displacement served as the controller input variables. In addition, the operating region of contactor, and the upper and the lower force-error limitations are determined by the armature displacement. As the change in the armature displacement, the programming of hysteresis comparator is changed as well.

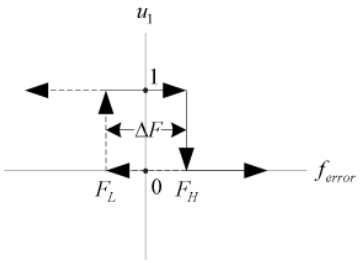

Fig. 12. Programs the hysteresis-comparator in the armature displacement estimator.

Fig. 12 illustrates the hysteresis-programming of the armature displacement estimator, and the upper and lower force-error definitions in individual operating region is expressed in terms of the armature displacement as follows:.

(1) Accleration region ($0 < x \le x_i$): $F_H = 12$ N, $F_L = 0$ N

(2) Decleration region ($x_i < x \le x_j$): $F_H = 0$ N, $F_L = -2$ N,

(3) Holding region ($x > x_j$): $F_H = F_L = 0$ N.

5.1 Verification of Estimator's Feasibility

In case of both the coil current and the armature displacement is known, the other contactor parameters can be calculated as well. If and only if the estimated armature displacement $\hat{x}$ and the coil current value i' are agree well with those measured from the real ac contactor, it means the accuracy of the proposed ADE is acceptable. This result also ensures that proposed ADE is feasible. It can replace the conventional sensors needed situation. By using a testing rig shown in Fig. 7 for validation the feasibility of ADE, the measured armature displacement of an ac contactor x and the simulated armature displacement $\hat{x}$ are together diagrammed in Fig. 13. We found these two armature- displacement curves are in good agreement. Moreover, the change of the coil current in the real contactor is basically the same as that in the estimator, as shown in Fig. 14.

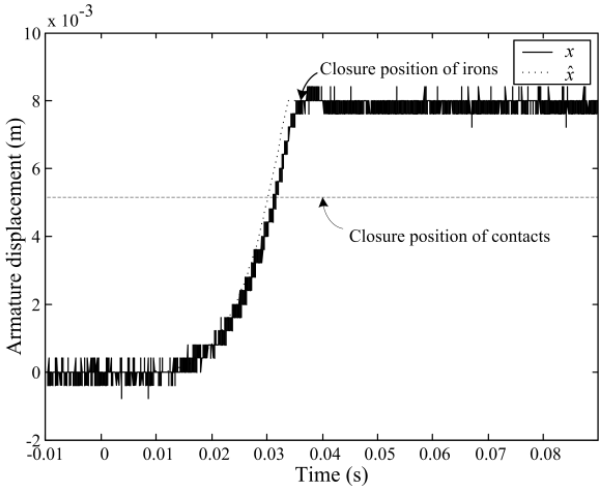

Fig. 13. Armature positions of the real contactor and estimator (Notice the contact occurs to close at 32 msec after the closing phase starts.

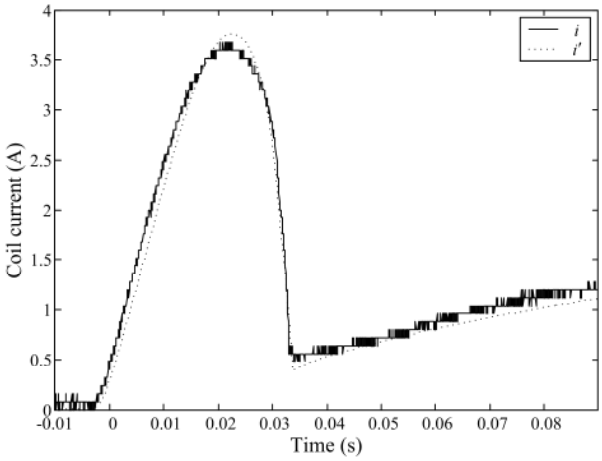

Fig. 14. Coil current values which are produced by the real contactor and the estimator respectively.

5.2 Verification of Estimator's Robustness

The proposed sensorless close-loop closing control of an ac contactor is based on the ADE. However, to avoid the proposed closing control is affected by the variation of the interior parameters. In the following, there are two different experiments were considered in terms of the variation of the armature mass and the spring coefficient. The effects of these two parameters upon the behavior of the armature displacement estimator will be examined and discussed.

As we known, in general, the motion of the mechanical system for a contactor can be described by using the Newton's motion law. The moving displacement of the armature is commonly determined by the force error f_{error}, which acts on the armature during closing process, and the

armature mass m . Initially, let the mass of the armature be M (m =0.265 Kg), and the armature mass possibly becomes light due to the interior factors, such that friction force is reduced due to continual working. Therefore, the other three different armature masses are assumed to be occurred, for example, M1 (m =0.235 Kg), M2 (m =0.245 Kg), and M3 (m =0.255 Kg). The dynamic performances of the ADE were measured and evaluated in terms of the armature displacement, moving velocity, coil current and electromagnetic force under the sensorless closing close-loop control. No matter how the armature mass is changed, Fig. 15 shows the final estimated armature displacement is almost nothing affected by the armature mass changed. In the lighter armature mass case, Figs. 16 and 17 depicts the contactor has much more coil current and the armature moving velocity than that of the initial armature mass M case. As the Fig. 18 shows that the lower the armature mass there is, the larger the electromagnetic force value will be. From the changing trend of the coil current and armature moving velocity is going to decrease the armature-displacement difference between with and without the armature mass changed. Experimental results show that the sensorless close-loop closing control of ac contactor, which is combined with the proposed ADE, has a very outstanding robust capability.

In a contactor spring system, in addition to the return springs, in general, one or triple sets of contact springs are included. In the initial closing stage of the contactor, only the return springs will be compressed till the contacts are closed. Next, the over-distance displacement of armature starts, both the return springs and contact springs are compressed together. The spring system is the main counter-force contributor which acts on the armature in the closing process, and it can be expressed as

$$f_f = \begin{cases} 2k_1x_1 + 2a \\ \quad at \;\; 0 \le x = x_1 \le 0.005194) \\ (2k_1 + 3k_2)x_2 + 2a + 3b \\ \quad at \;\; 0.005194 \le x = x_2 \le 0.008 \end{cases} \qquad (35)$$

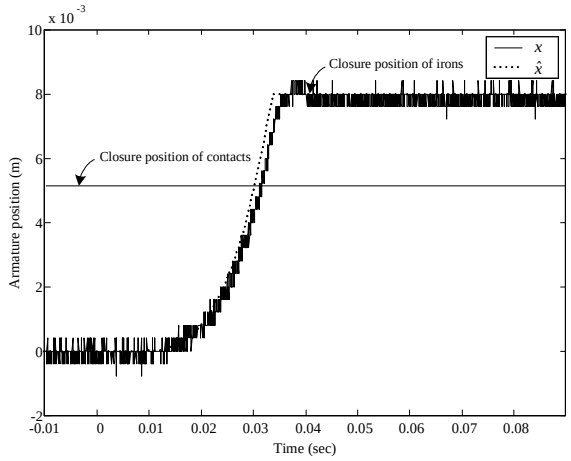

Fig. 13. Armature positions of the real contactor and estimator (Notice the contact occurs to close at 32 msec after the closing phase starts.

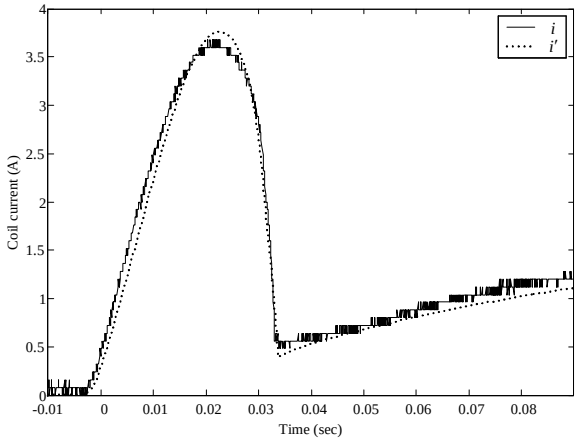

Fig. 14. Coil current values which are produced by the real contactor and the estimator respectively.

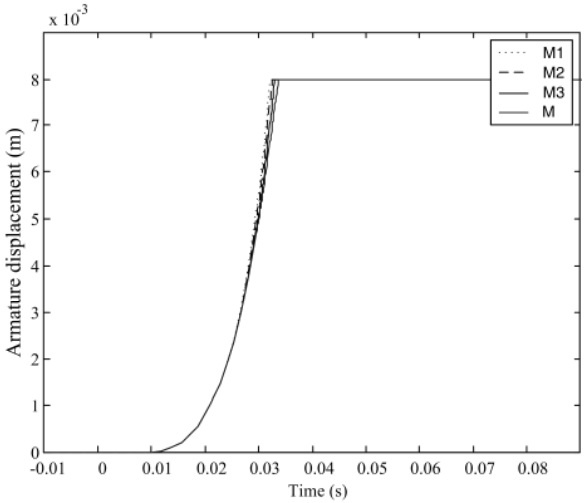

Fig. 15. Armature position with respect to time curve under different armature masses.

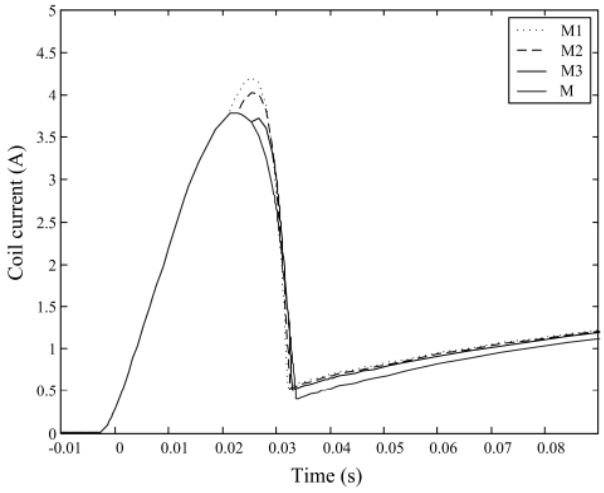

Fig. 16. Coil current with respect to time curve under different armature masses.

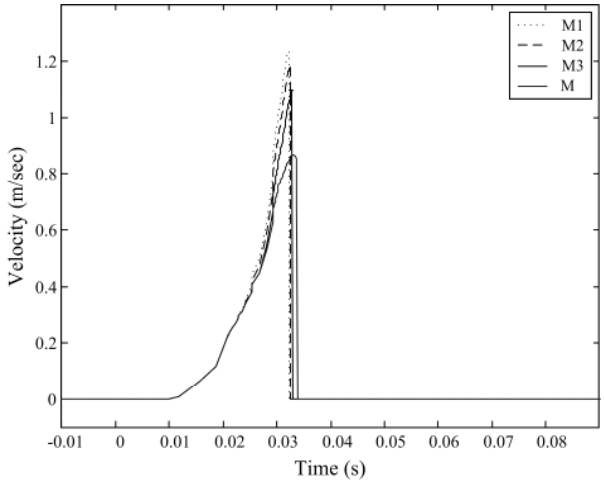

Fig. 17. Armature moving velocity with respect to time curve under different armature masses.

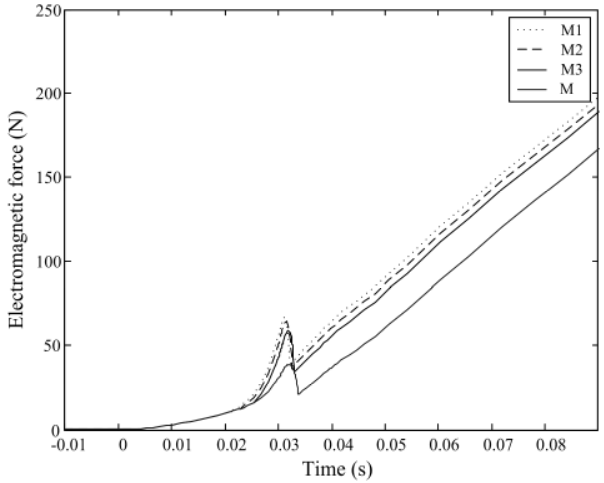

Fig. 18. Magnetic force with respect to time curve under different armature masses.

where k_1 is the spring coefficient and $k_1 = 4.39968 \times 10^2$ N/m, a is the initial pressure of spring and $a = 0.25$ N, k_2 is the contact spring's coefficient and $k_2 = 1.71405 \times 10^3$ N/m, and b is the initial pressure of contact springs and $b = 8.36667$ N. Let above-mentioned assumptions be condition K, another three cases are respectively assumed to be as follows

(1) condition $K1$: $k_1 - 100, k_2 = k_2 - 300$,

(2) condition $K2$: $k_1 - 200, k_2 = k_2 - 600$,

(3) condition $K3$: $k_1 - 300, k_2 = k_2 - 900$.

The less the spring coefficient has, the smaller spring anti-force is. The armature-displacement error becomes larger too. To reduce the armature-displacement error of the proposed sensorless close-loop closing control system as possible as, as shown in Figs. 20 and 22, the response of the estimator is to increase the value of the coil current, thus the strength of the electromagnetic force acts on the armature is then increased as well. Fig. 21 indicates that there is a short time interval; the armature moving velocity is suddenly increased. The final armature displacement of the estimator is almost nothing affected by the change of the spring coefficients too; this result is shown in Fig. 19.

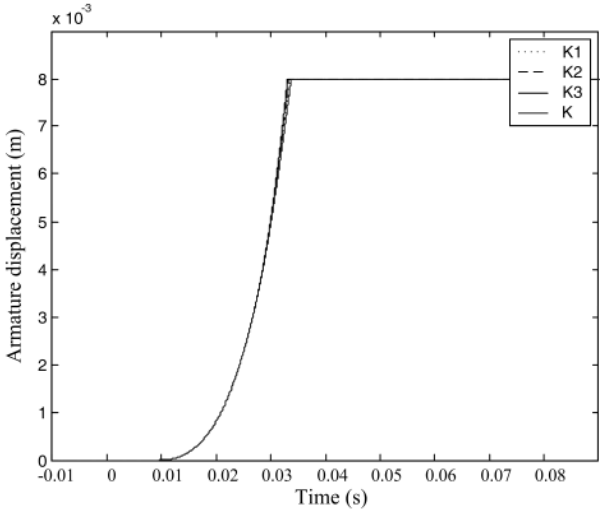

Fig. 19. Armature position with respect to time curve under different spring constants.

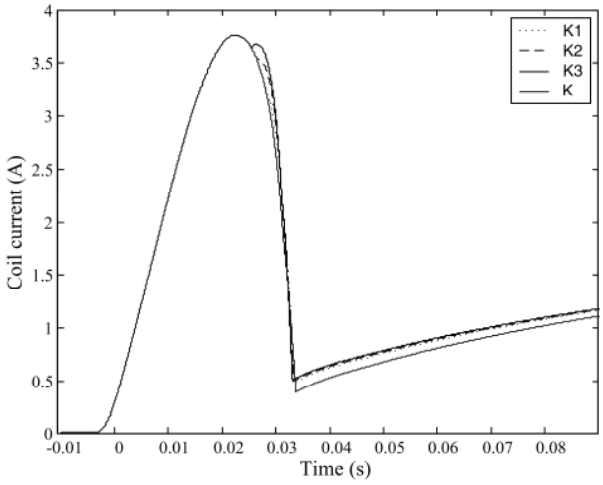

Fig. 20. Time-varying coil current curves with various spring coefficients.

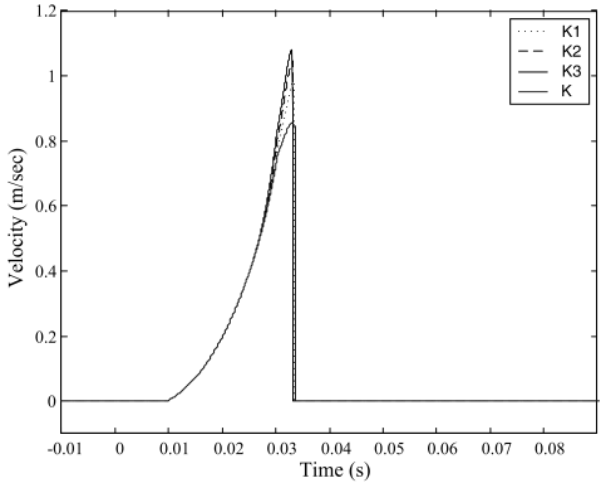

Fig. 21. Time-varying armature velocity curve with various spring coefficients.

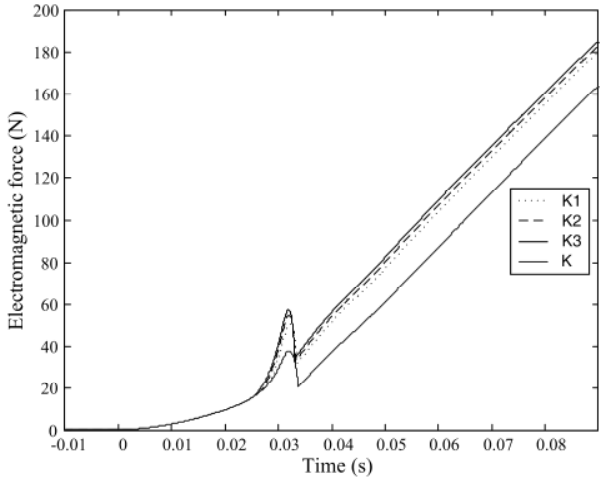

Fig. 22. Time-varying electromagnetic force curve with various spring coefficients.

5.3 Testing Bounce Duration

Fig. 23 is the testing rig for the measurement of the number of contact bounce after contacts closing during the closing process. Each one set of contact has two terminals. One of the terminals is connected to a dc voltage source, +5 V, while the other terminal is connected to the ground through a fixed resistor R. When the contacts are closed together, a dc voltage level 5 V across the fixed resistor is measured through the testing point TP by using the digital scope. Otherwise, when the contacts are disconnected, thus, the voltage across the testing point TP will be set to be zero.

The upper waveform in Fig. 24 denotes the measured contact bounce under the contactor is without control and directly supplied with a dc voltage source 24 V. Contact bounces are repeated after contacts closing. In contrast, fewer or even no contact bounces occur to the ac contactor which is controlled by the proposed sensorless close-loop closing control method. However, we found the first contact closure time with control case is apparently lagging without control case by approximately about 15 msec.

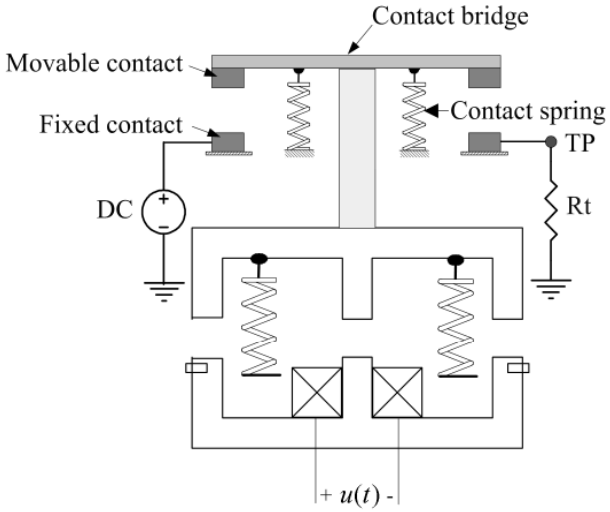

Fig. 23. Testing rig for measuring the bounce duration after contacts closing.

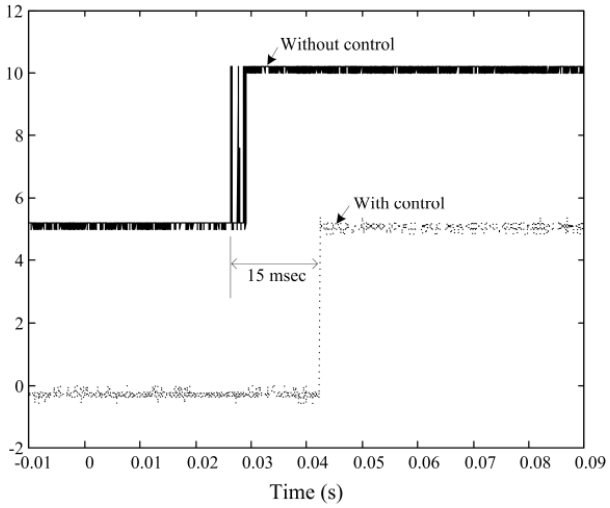

Fig. 24. Bouce-duration comparison between with and without proposed control conditions. (Vertical: 2 V/div)

6 Conclusion

The objective of this paper is focused on developing a new ADE. As long as the coil current and the coil voltage data are well-known, the instantaneous estimated armature displacement can be calculated. The proposed armature displacement features its simplicity and robustness. The effects of interior parameters' variation, such as the armature mass and spring coefficient, upon the robust capability of the estimator are considered. Experimental results show that the

robust capacity of ADE is very outstanding. Furthermore, if the proposed ADE is combined with a hysteresis controller, a sensorless closing control strategy is implemented in the control board for the reduction of bounce duration after contacts closing. Experimental results indicate the bounce duration is shorter than that of conventional ac contactor. Bouncing phenomenon is sometimes even completely being eliminated.

References:

[1] X. Zhou, L. Zou, and E. Hetzmannseder, Asynchronous Modular Contactor for Intelligent Motor Control Applications, *Proceedings 51st Meeting IEEE Holm Conference on Electrical Contacts*, 2005, pp. 55–62.

[2] J. H. Choi, J. M. Kwon, J. H. Jung, and B. H. Kwon, High-Performance Online UPS Using Three-Leg-Type Converter, *IEEE Transactions on Industry Electron*, Vol.52, No.3, Jun. 2005, pp. 889–897.

[3] D. A. R. Lopes, E. G. de Jesus, and L. A. F. Valle, Maintaining the Continuity of Process Operation after Voltage Sag or Power Interruption, *Proceedings 51st Annual Conference on Petroleum and Chemical Industry Technical*, Sept. 2004, pp. 81-86.

[4] H. Manhart and W. Rieder, Erosion Behavior and Erodibility of AgCdO and AgSnO2 Contacts Under AC3 and AC4 Test Conditions, *IEEE Transactions on CPMT*, Vol.13, Mar. 1990, pp. 56-64.

[5] W. Rieder and V. Weichsler, Make Erosion on Ag/SnO2 and Ag/CdO Contacts in Commercial Contactors, *Proceedings of the 46th IEEE Holm Conference on Electrical Contacts*, Aug. 1990, pp. 110–116.

[6] H. Nouri, F. Kalvelage, T. S. Davies, and J. H. Kiely, Erosion Dependency of 3-phase Contactor Contacts on Configuration of Loads, *Proceedings of the 46th IEEE Holm Conference on Electrical Contacts*, Sept. 2000, pp.153 – 160.

[7] T. S. Davies, H. Nouri, and F. Britton, Towards the Control of Contact Bounce, *IEEE Transactions on CPMT*, Vol.19, No.3, Sept. 1995, pp. 353-359.

[8] H. Nouri, N. Larsen, and T. S. Davies, Contact Bounce Simulation Using MATLAB, *Proceedings of the 43rd IEEE Holm Conference on Electrical Contacts*, Oct. 1997, pp. 184-288.

[9] W. Li, J. Lu, H. Guo, and X. Su, AC Contactor Making Speed Measuring and Theoretical Analysis, *Proceedings of the 50th IEEE Holm Conference on Electrical Contacts*, 2004, pp. 403–407.

[10] X. Su, J. Lu, B. Gao, G. Liu, and W. Li, Determination of the Best Closing Phase Angle for AC Contactor Based on Game Theory, *Proceedings of the 52nd IEEE Holm Conference on Electrical Contacts*, Sept. 2006, pp. 188 – 192.

[11] X. Zhihong and Z. Peiming, Intelligent Control Technology of AC Contactor, *Proceedings of the IEEE/PES Transmission Distribution Conference Exhibition: Asia Pacific*, 2005, pp. 1–5.

[12] A. G. Espinosa, J.-R. R. Ruiz, and X. A. Morera, A Sensorless Method for Controlling the Closure of a Contactor, *IEEE Transactions on Magnetics*, Vol. 43, Oct. 2007, pp. 3896–3903.

[13] T. Roschke, Electronic Control of Electromagnetic Contactors, *Proceedings of the 19th ICEC*, pp. 295–299, 1998.

[14] G. Griepentrog, F. Kalvelage, N. Elsner, and N. Mitlmeier, Increase of Lifetime of Electromagnetically Actuated Contactors by Avoiding Self-Synchronization, *Proceedings of the 50th IEEE Holm Conference Electrical Contacts*, 2004, pp. 408–415.

[15] A. A. Slonim, Bouncing of Contacts under Current Load (the Influence of Mechanical System Parameters and Load Current on the Closing Process of Electrical Contacts), *IEEE Transactions Components., Hybrids, Manufacturing Technology*, Vol.CHMT-10, No.1, Mar. 1987, pp. 122–126.

[16] C. T. Chi, A Study of Closing Adaptive Control in Electronically Controlled Intelligent Contactor, *Proceedings of the IEEE Region 10 Conference TENCON*, Nov. 2006, pp. 1–4.

[17] S. Camur, B. Arifolu, E. K. Beber and E. Beþe, Application of Semiconductor Compensation Contactor Improved for Sensitive and Fast Compensation System, *WSEAS Transactions on Power Systems***,** Issue 2, Vol.1, Feb. 2006, pp. 381-386.

[18] M. Andriollo, G. Bettanini, G. Martinelli, A. Morini, S. Stellin and A. Tortella, Electromagnetic Design of In-wheel Permanent Magnet Motors, *WSEAS Transactions on Power Systems*, Issue 2, Vol.1, Feb. 2006, pp. 303-310.

[19] H. Davis and R. Robert, *Fundamental of Physics*, Taiwan, John Wiley & Sons Inc., 1981.

[20] T. Kato and K. Miyao, Modified Hysteresis Control with Minor Loops for Single-Phase Full-Bridge Inverters, *IEEE Industry Application Society Annual Meeting*, Vol.1, Oct. 1988, pp. 689- 693.

[21] S. Janne, H. Marko, and L. Jorma, Sensorless Control of Induction Motor Drives Equipped with Inverter Output Filter, *IEEE Transactions on Industry Electronic*, Vol.53, No.4, Aug. 2006, pp.1188-1190.